ECCOMAS Congress 2016
VII European Congress on Computational Methods in Applied Sciences and Engineering
M. Papadrakakis, V. Papadopoulos, G. Stefanou, V. Plevris (eds.)
Crete Island, Greece, 5–10 June 2016

MODELLING THERMAL BARRIER COATINGS AND THEIR INFLUENCE ON THE LIFETIME OF ROCKET ENGINE NOZZLE STRUCTURES

Marek Fassin, Stephan Wulfinghoff, and Stefanie Reese

Institute of Applied Mechanics
Mies-van-der-Rohe-Str.1, D-52074 Aachen (Germany)
e-mail: {marek.fassin,stephan.wulfinghoff,stefanie.reese}@rwth-aachen.de

Keywords: viscoplasticity, damage, thermal barrier coating, lifetime prediction

Abstract. *The walls of rocket engine nozzle structures undergo extreme thermomechanical loadings during the engine cycle. These loads cause an accumulation of plastic strains due to creep and relaxation which finally lead to the failure of the hot gas wall. One approach to increase the lifetime of the hot gas wall is the reduction of the temperatures in the hot gas wall since the temperature is the main driver of this failure phenomenon. Special thermal barrier coating (TBC) systems are under development in order to protect the copper alloy of the hot gas wall from high temperatures. The present paper studies the influence of such thermal barrier coatings regarding the damage behaviour of the hot gas wall made of a copper alloy. In the first step, thermal analyses are performed to define an appropriate TBC thickness and the needed coolant power such that the maximum service temperature of the TBC is not exceeded. Furthermore the temperature distributions of the hot gas wall with and without TBC are compared, which show a reduction in temperature of approximately* 200 *K. In the second step static analyses with a recently developed viscoplastic damage model are presented. Here damage distributions as well as the deformation behaviour of the hot gas wall with and without TBC are compared. It is shown that the application of TBCs has an positive effect on the damage behaviour as well as the deformation of the hot gas wall.*

1 INTRODUCTION

The demand for higher payloads and the general endeavour of a performance increase of rocket engines require the development of reliable lifetime prediction models. During the operation of the rocket engine the hot gas wall undergoes extreme cyclic thermomechanical loads. These cyclic loads lead to an accumulation of plastic strains, followed by thinning and bulging of the hot gas wall. Finally, after several cycles the hot gas wall (usually made of a copper alloy) fails (see Figure 1). Since the deformed hot gas wall resembles the shape of a doghouse, the failure mode is called doghouse effect (see e.g Riccius et al. [1]). This failure phenomenon can be rather related to ductile damage than to low cycle fatigue (see e.g. Schwarz et al. [2]). One

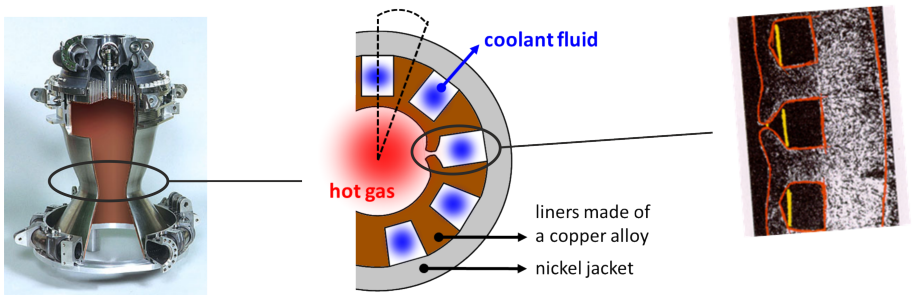

Figure 1: Left: Combustion chamber of the Vulcain rocket engine, Center: schematic cross section of the combustion chamber, Right: microscopic picture of the doghouse effect [1].

approach to increase the lifetime of the hot gas wall is the reduction of the temperatures in the hot gas wall. This seems to be a reasonable idea since the damage and failure behaviour of the copper alloy/copper substrate is highly temperature dependent. Special thermal barrier coating (TBC) systems for the application on copper alloys have been developed by the Institute for Materials at TU Braunschweig in order to protect the copper alloy from extremely high temperatures [3, 4, 5, 6, 7, 8, 9]. A thermal barrier coating typically consists of two layers: a bond coat and a top coat. In previous studies of the Institute for Materials [3, 4, 5, 6] a coating system usually used in gas turbines was investigated (bond coat: NiCrAlY, top coat: yttria-stabilized zirconia). However, this system turned out not be practical since the coatings failed at the bond coat/copper substrate interface due to (i) mismatch of the coefficient of thermal expansion (CTE) and (ii) the chemical gradient between the copper alloy substrate and the bond coat [5]. Therefore, a new bond coat NiCuCrAl was developed offering higher chemical similarity to the substrate as well as reducing the mismatch in the CTE. The current promising thermal barrier coating system is composed of a NiCuCrAl bond coat and a NiCrAlY top coat (see Fiedler et al. [8, 9]).

Butler and Pindera [10] investigated as one of the first the influence of thermal barrier coatings on the doghouse effect. They found that by the application of TBCs the temperature distribution within the hot gas wall was dramatically changed and reduced. They concluded that the strongly temperature dependent creep/relaxation of the copper alloy which is one of the main reasons for the doghouse failure can be limited by TBCs. By utilizng a viscoplastic material model they showed that the thickness of the TBC directly influences the deformation of the hot gas wall. Fiedler et al. [9] investigated with FE-simulations based on a micro model the interface stresses between the copper substrate and the bond coat. As desired, the interface stresses perpendicular to the surface are reduced strongly compared to the former bond coat made of NiCrAlY. Furthermore a temperature reduction in the copper substrate of approximately 200 K was observed.

The present study focuses on the lifetime of the copper alloy (which shall be increased by the application of a TBC), not on the lifetime of the TBC. Figure 2 left shows the representative segment of the cooling channel structure, which is highlighted in Figure 1 (center) by the dashed line, with the additional TBC on the hot gas wall (marked in red). Figure 2 (center) shows the FE model of the corresponding finite element model, where the TBC is discretized with several elements over the thickness. In reality, the TBC is a system of two layers: a top coat and a bond coat. Due to simplicity and the similarity of the thermal and mechanical properties of the two layers, the present study merges the two layers to one layer called "TBC" in the following. This approach is considered to be sufficient for the investigation of the lifetime/behavior of the subjacent copper alloy.

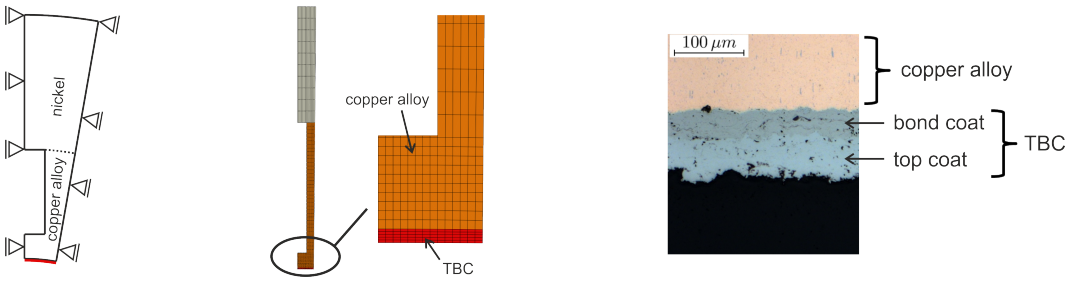

Figure 2: Left: segment of the cooling channel structure with TBC on the hot gas wall (marked in red), Center: FE model of the cooling channel segment with TBC, Right: microscopic picture of a TBC applied on a copper alloy [11].

2 MATERIAL MODELLING

The material model utilized for the lifetime investigations of the copper alloy has been developed and presented in previous works (see e.g. Tini et al. [12] and Kowollik et al. [13]). Therefore the material model is only briefly summarized and for more details it is referred to the latter mentioned publications. In order to take into account the relevant phenomena occuring during the thermomechanical loading of the copper alloy hot gas wall a viscoplastic material model considering isotropic damage is used. The corresponding rheological model is depicted in Figure 3. Schwarz et al. [14] compared isotropic damage models with anisotropic damage models (with and without considering micro defect closure effects) and concluded that neither damage anisotropy nor the crack closure effect strongly affect the global failure phenomenology. Due to this reason and to keep the number of parameters as low as possible the isotropic damage model is considered to be sufficient to perform first studies on the influence of the thermal barrier coatings on the lifetime of the copper alloy. An anisotropic damage model has been already developed by the authors (see e.g. Fassin et al. [15]) and was furthermore applied for lifetime simulations of rocket combustion chamber walls (see Fassin et al. [16] and Wulfinghoff et al. [17]). The intent of the authors for the future is also to use anisotropic damage models for simulations involving thermal barrier coatings.

The thermomechanical material parameters for the copper alloy are chosen according to Kowollik et al. [13] with the only difference that the coefficient of thermal expansion is adopted from Baeker et al. [18] to be now temperature dependent. The nickel material behaviour only plays a minor role and is therefore modelled as linear elastic (cf. Kowollik et al. [13]). The material behaviour of the TBC is modelled by an ideal elastoplastic material law as it was already done

in Baeker et al. [18]. The material parameters for the TBC were adopted from the bond coat material (NiCuCrAl).

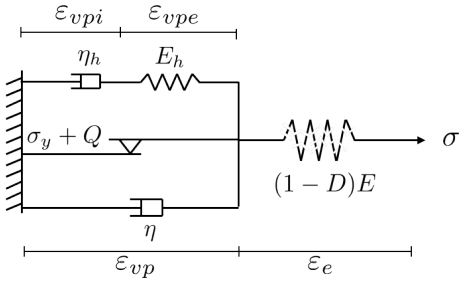

Figure 3: Rheological model of the viscoplastic material model incorporating isotropic damage.

Table 1: Summary of the constitutive equations of the viscoplastic damage model.

total strain	$\boldsymbol{\varepsilon}$	=	$\boldsymbol{\varepsilon}_e + \boldsymbol{\varepsilon}_{vp} + \boldsymbol{\varepsilon}_{th}$
effective elasticity tensor	$\widetilde{\mathbf{C}}$	=	$(1-D)\,\mathbf{C}$
stress	$\boldsymbol{\sigma}$	=	$\widetilde{\mathbf{C}}\,[\boldsymbol{\varepsilon}_e]$
effective stress	$\widetilde{\boldsymbol{\sigma}}$	=	$\mathbf{C}\,[\boldsymbol{\varepsilon}_e]$
back stress deviator	$\boldsymbol{X}^D$	=	$2\mu_h\left[\boldsymbol{\varepsilon}^D_{vpe}\right]$
total strain	$\boldsymbol{\varepsilon}$	=	$\boldsymbol{\varepsilon}_e + \boldsymbol{\varepsilon}_{vp} + \boldsymbol{\varepsilon}_{th}$
viscoplastic strain	$\boldsymbol{\varepsilon}_{vp}$	=	$\boldsymbol{\varepsilon}_{vpe} + \boldsymbol{\varepsilon}_{vpi}$
yield function	Φ	=	$\left\|\widetilde{\boldsymbol{\sigma}}^D - \boldsymbol{X}^D\right\| - \sqrt{\frac{2}{3}}\,(\sigma_y + Q)$
viscoplastic strain rate	$\dot{\boldsymbol{\varepsilon}}_{vp}$	=	$\dfrac{\dot\lambda}{1-D}\,\dfrac{\widetilde{\boldsymbol{\sigma}}^D - \boldsymbol{X}^D}{\left\|\widetilde{\boldsymbol{\sigma}}^D - \boldsymbol{X}^D\right\|}$
(local inelastic) viscoplastic strain rate	$\dot{\boldsymbol{\varepsilon}}_{vpi}$	=	$\dot\lambda\, b\, \boldsymbol{\varepsilon}^D_{vpe}$
damage	$\dot D$	=	$\dot p\,\left(\frac{Y}{S}\right)^k\, H_{(p-p_D)}$
plastic multiplier	$\dot\lambda$	=	$\dfrac{\langle\overline{\Phi}\rangle^m}{\eta}$

3 THERMAL ANALYSIS

The basis of the transient thermal analysis is Fourier's heat equation

$$\Delta T = \frac{\rho c}{\zeta}\frac{\partial T}{\partial t}, \tag{1}$$

with temperature T and time t. Here, the material parameters are ρ (density), c (heat capacity) and ζ (thermal conductivity). For the values of the material parameters of the copper alloy

and nickel, see Fassin et al. [16]. For the TBC the material parameters of NiCuCrAl from Baeker et al. [18] are used. The finite element model of the cooling channel segment with TBC used for the thermal as well as for the static analysis is shown in Figure 4. The thermal boundary conditions are described in the following: The interaction with the cooling fluid in the cooling channel and the hotgas on the hot gas wall is modelled via convective boundary conditions. For the cooling fluid the heat transfer coefficient α_{cf} and the bulk temperature T_{cf} are prescribed, for the hot gas boundary condition α_{hg} and T_{hg}. One engine cycle consists of a pre cooling, a hot run, a post cooling and a relaxation phase, for which the corresponding values are listed in Table 3. A special case is present for the heat transfer coefficient α_{hg} on the hot gas wall surface. This value is dependent on the wall temperature T_w of the hot gas wall and was adopted from Baeker et al. [18]. For the heat transfer coefficient of the cooling fluid values varying between $50\,\mathrm{kW/(m^2K)}$ and $60\,\mathrm{kW/(m^2K)}$ are applied. This variation corresponds to a varying mass flow rate of the cooling fluid. For the other free surfaces of the segment adiabatic boundary conditions are applied. In order to illustrate the influence

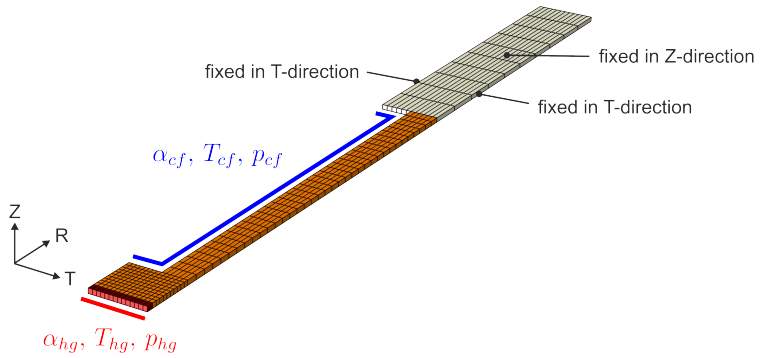

Figure 4: Finite element model of the cooling channel segment with TBC with thermal and static boundary conditions.

Phase	**Time**	**Hot gas**		**Cooling channel**	
[-]	t [s]	$\alpha_{hg}\left[\frac{\mathrm{kW}}{\mathrm{m^2K}}\right]$	T_{hg}[K]	$\alpha_{cf}\left[\frac{\mathrm{kW}}{\mathrm{m^2K}}\right]$	T_{cf}[K]
Pre cooling	0-2	$f(T_w)$	293.15	50...60	50
Hot run	2 - 602	$f(T_w)$	3435	50...60	50
Post cooling	602 - 604	$f(T_w)$	293.15	50...60	50
Relaxation	604 - 1000	$f(T_w)$	293.15	0.15	293.15

Table 2: Thermal boundary conditions for the hot gas and the cooling channel in one engine cycle.

of the thickness of the TBC on the temperature in the hot gas wall, several parameter studies have been performed. The conducted thermal analyses encompassed in each case only one engine cycle since the temperature distribution is approximately the same in every cycle. First of all, an appropriate TBC thickness and cooling fluid coefficient have to be specified to limit the maximum temperatures occuring in the TBC. Therefore transient thermal analyses were performed with different TBC thicknesses and cooling fluid heat transfer coefficients α_{cf}. For the design of the TBC system the maximum occuring temperature on the surface of the TBC is an important value since it has to be under the maximum service temperature of the TBC, which is around 1500 K for NiCuCrAl. Figure 5 shows the maximum temperature occuring on

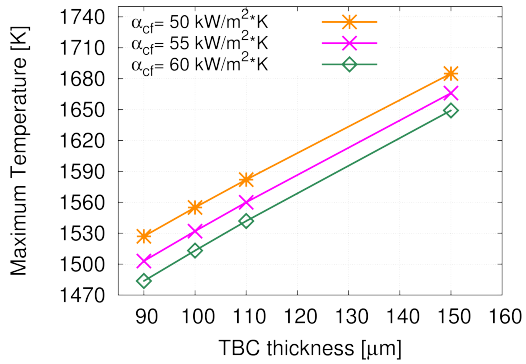

Figure 5: Maximum temperature occuring on the surface of the TBC in dependence of the thickness of the TBC for different heat transfer coefficients.

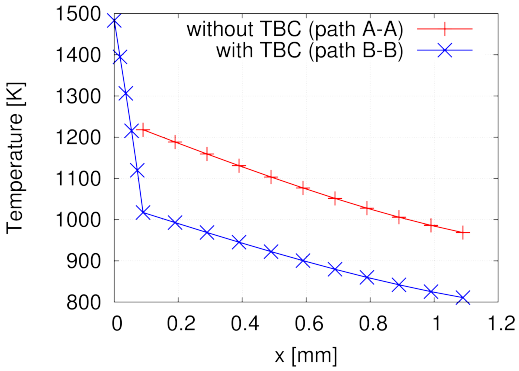

Figure 6: Comparison of the temperature distribution within the hot gas wall along the distance x for the versions "without TBC" and "with TBC".

the surface of the TBC in dependence of the thickness of the TBC for different heat transfer coefficients α_{cf}. It can be seen that the thicker the TBC, the higher is the maximum occuring temperature. This can be explained by the insulation effect of the TBC, which has a much lower thermal conductivity than the copper alloy. Therefore the thermal resistance increases with increasing TBC thickness which leads to a lower heat flux through the hot gas wall. This finally results in a higher surface temperature. Figure 5 shows that only for a TBC thickness of t=90 μm and for a strong cooling with α_{cf}=60 $\mathrm{kW/(m^2K)}$ the maximum occuring temperature lies under 1500 K. For this reason the further discussion of the results of the thermal analyses focus on this configuration. The static analyses in Section 4 will be also performed with this configuration.

In Figure 7 the temperature contour plots for the hot gas wall at the end of hot run (t=602 s) for the versions "without TBC" and "with TBC" are opposed to each other. Due to the application of the TBC, the temperature in the copper alloy could be drastically decreased. In contrast to that, the maximum occuring temperature on the TBC surface (T=1483 K) is much higher than the maximum occuring temperature on the hot gas wall surface for the version "without TBC" (T=1218 K). The strong temperature decrease within the TBC, which is approximately linear, is illustrated in Figure 6. Five elements over the thickness of the TBC were applied, which is shown by the six nodal temperatures plotted for path B-B for the first 0.09 mm (thickness of the TBC). The main purpose of the TBC, the reduction of the temperature within the copper alloy, is clearly depicted. The temperature reduction (difference between the red and the blue line) is round about 200 K. The maximum occuring temperature in the copper alloy is reduced from 1218 K to 1017 K. The surface temperature on the cooling channel wall is reduced from 969 K to 811 K. This temperature reduction is seen to be very promising to increase the lifetime of the copper alloy hot gas wall, which will be investigated in the next section.

4 STATIC ANALYSIS

The temperature field of the segment at every time point is used as input for the series of quasi static analyses with which the lifetime of the copper alloy will be investigated. The material parameters are temperature dependent as described in Section 2. Furthermore the thermal expansion of the material plays a major role in the static simulation, which is considered by the thermal strain. The static boundary conditions of the cooling channel segment are described in Figure 4. The left and the right face of the segment are fixed in tangential direction (T-direction)

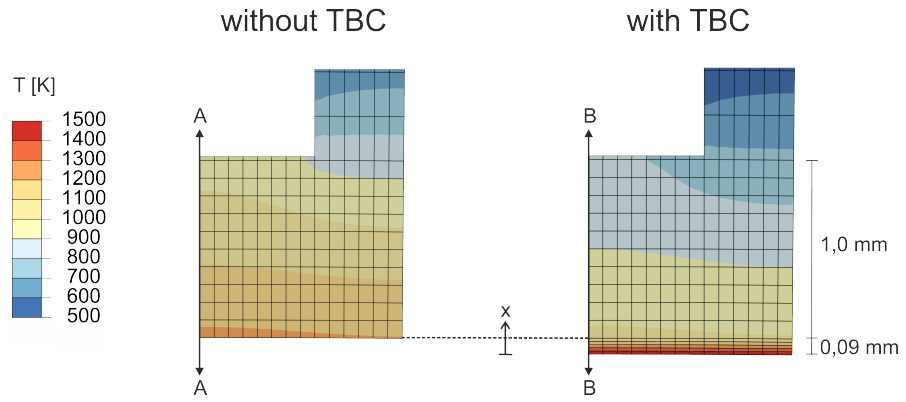

Figure 7: Temperature contour plots for the hot gas wall at the end of hot run (t=602 s) for the versions "without TBC" and "with TBC".

due to rotational symmetry. In thickness direction (Z-direction) a generalized plane strain condition is enforced (all elements in the R-T plane have the same strain in Z-direction) where the upper face is fixed in Z-direction and the bottom face is free. The boundary conditions of the cooling channel wall and the hot gas wall are given by means of pressures (see Table 4). For the finite element simulations 8-node bricks with reduced integration and hourglass stabilization are utilized. The time stepping is set manually. Figure 8 shows the damage distributions in the

Phase [-]	**Time** t [s]	**Hot gas pressure** p_{hg} [MPa]	**Coolant pressure** p_{cf} [MPa]
Pre cooling	0 - 2	0	20
Hot run	2 - 602	10	20
Post cooling	602 - 604	0	20
Relaxation	604 - 1000	0	0

Table 3: Hot gas and coolant pressure over one engine cycle.

hot gas wall for the versions "without TBC" and "with TBC" after 10 and 20 cycles. After 10 cycles (cf. Figure 8(a)) the bulging of the hot gas wall is already clearly visible. For the version "without TBC" the highest values of the isotropic damage variable D occur at the corner of the cooling channel and at the hot gas side in the middle of the fin. Furthermore damage has also accumulated in the center of the ligament. In contrast, the version "with TBC" shows mainly damage at the corner of the cooling channel and no further pronounced places of damage accumulation as for the version "without TBC". After 20 cycles (cf. Figure 8(b)) the deformation and the damage in the hot gas wall have further evolved. The differences between the damage distributions for the version "without TBC" and "with TBC" are the same as described already for the distributions after 10 cycles. In summary, it can be stated that the damage for the version "with TBC" is, as expected, smaller than for the version "without TBC". However, the differences in the maximum values of the isotropic damage varibale D are smaller than expected. The influence of the TBC becomes more apparent in terms of deformation. The deformation of the hot gas wall (after 10 cycles as well as after 20 cycles) is higher for the version "without TBC". This is illustrated by the comparison of the displacement difference $\Delta u_{y,1-2}$ of node 1 and 2 with the displacement difference $\Delta u_{y,3-4}$ of node 3 and 4, which are measures for the

bulging of the hot gas wall. Figure 9 shows this deformation over the calculated 20 cycles. By using a TBC the deformation after 20 cycles is reduced by 30 %.

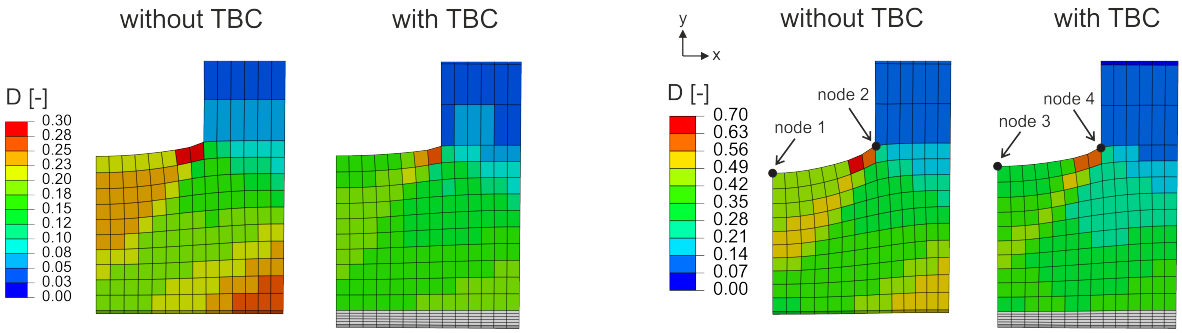

(a) after 10 cycles. (b) after 20 cycles.

Figure 8: Comparison of the damage distributions in the hot gas wall for the versions “without TBC” and “with TBC” after 10 and 20 cycles.

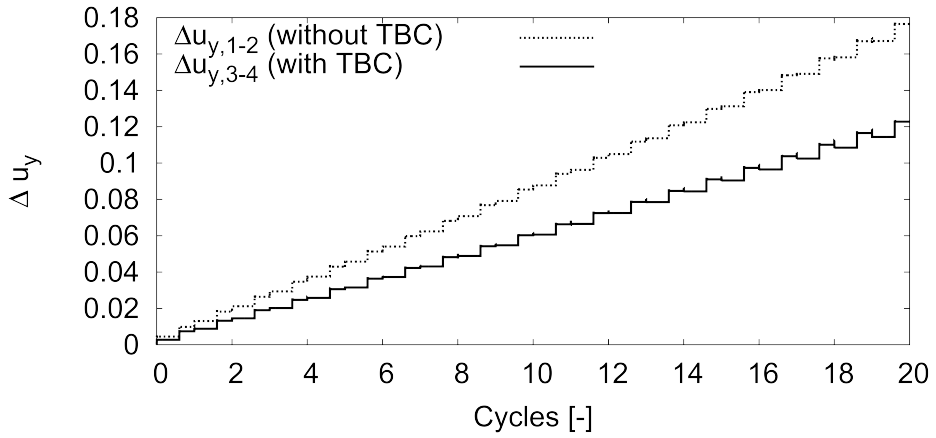

Figure 9: Comparison of the displacement differences $\Delta u_{y,1-2}$ and $\Delta u_{y,3-4}$.

5 CONCLUSIONS

In this work the influence of thermal barrier coatings on the lifetime and deformation behaviour of rocket engine nozzle structures made of copper alloys has been investigated. For the material modelling of the copper alloy a viscoplastic material model incorporating isotropic damage was applied. As input for the series of quasi static analyses including 20 cycles, the temperature field for one engine cycle was used repeatedly. In the first step an appropriate TBC thickness and the needed cooling fluid heat transfer coefficient were defined such that the maximum service temperature of the TBC was not exceeded. Afterwards it was shown that with the defined configuration (t_{TBC}=90 μm and α_{cf}=60 kW/(m^{2}K)) a temperature reduction of approximately 200 K is obtained. The evaluation of the static simulations of 20 cycles showed that the damage distribution for a hot gas wall with TBC is slightly different from the one without TBC. The damage for the version “with TBC” was, as expected, smaller than for the version

"without TBC". However, the differences regarding the maximum values of the isotropic damage varibale D were smaller as expected. But it was revealed that the deformations of the hot gas wall (bulging of the hot gas wall) induced by the thermomechanical loading were less pronounced when a TBC was applied.

Acknowledgements

Financial support provided by the German Research Foundation (DFG) within the projects TPD3 and TPD2 of the CRC/Transregio 40 'Fundamental Technologies for the Development of Future Space-Transport-System Components under High Thermal and Mechanical Loads' is gratefully acknowledged.

REFERENCES

[1] Riccius JR, Haidn OJ, Zametaev EB. Influence of time dependent effects on the estimated life time of liquid rocket combustion chamber walls. *40th AIAA/ASME/SAE/ASEE Joint Propulsion Conference and Exhibit*, 2004.

[2] Schwarz W, Schwub S, Quering K, Wiedmann D, Höppel HW, Göken M. Life prediction of thermally highly loaded components: Modelling of the damage process of a rocket combustion chamber hot wall. *CEAS Space Journal* 2011; **1**:83–97, doi:10.1007/s12567-011-0007-9.

[3] Schloesser J, Fedorova T, Bäker M, Rösler J. Thermal barrier coating development for application in rocket engines. *SFB TRR40 Annual Report 2009*. Lehrstuhl fr Aerodynamik und Strmungsmechanik, Technische Universitt Mnchen, 2009.

[4] Schloesser J, Kowollik D, Bäker M, Rösler J, Horst P. Failure analysis and multiscale modeling of thermal barrier coatings. *SFB TRR40 Annual Report 2010*. Lehrstuhl fr Aerodynamik und Strmungsmechanik, Technische Universitt Mnchen, 2010.

[5] Schloesser J, Kowollik D, Bäker M, Rösler J, Horst P. Thermal barrier coatings in rocket engines - a multiscale simulation and development approach. *SFB TRR40 Annual Report 2011*. Lehrstuhl fr Aerodynamik und Strmungsmechanik, Technische Universitt Mnchen, 2011.

[6] Schloesser J, Kowollik D, Bäker M, Rösler J, Horst P. Sensitivity analyses and coating development of thermal barrier coatings in rocket engines. *SFB TRR40 Annual Report 2012*. Lehrstuhl fr Aerodynamik und Strmungsmechanik, Technische Universitt Mnchen, 2012.

[7] Fiedler T, Fedorova T, Rösler J, Bäker M. Design of a nickel-based bond coat alloy for thermal barrier coatings on copper substrates. *SFB TRR40 Annual Report 2013*. Lehrstuhl fr Aerodynamik und Strmungsmechanik, Technische Universitt Mnchen, 2013.

[8] Fiedler T, Rösler J, Bäker M. Development of a cunicral bond-coat for thermal barrier coatings in rocket combustion-chambers. *SFB TRR40 Annual Report 2014*. Lehrstuhl fr Aerodynamik und Strmungsmechanik, Technische Universitt Mnchen, 2014.

[9] Fiedler T, Rösler J, Bäker M. Design studies on thermal-barrier-coatings for liquid-rocket combustion-chambers. *SFB TRR40 Annual Report 2014*. Lehrstuhl fr Aerodynamik und Strmungsmechanik, Technische Universitt Mnchen, 2015.

[10] Butler Jr D, Pindera MJ. Analysis of factors affecting the performance of rlv thrust cell liners. *Technical Report*, NASA Glenn Research Center 2004.

[11] T. fiedler.

[12] Tini V, Kowollik D, Reese S, Haupt M. Application of a viscoplastic damage model for the failure prediction of regeneratively cooled nozzle structures. *ECCOMAS Coupled Problems 2011 Proceedings*, 2011.

[13] Kowollik D, Tini V, Reese S, Haupt M. 3d fluid-structure interaction analysis of a typical liquid rocket engine cycle based on a novel viscoplastic damage model. *International Journal for Numerical Methods in Engineering* 2013; **94chac**:1165–1190.

[14] Schwarz W, Wiedmann D, Schwub S, Höppel H, Göken M. Assessment of different continuum damage models for life-time prediction of high thrust cryogenic combustion chambers. *Proceedings of the 4th European Conference for Aerospace Sciences (EUCASS)*, 2011.

[15] Fassin M, Wulfinghoff S, Reese S. Different numerical time integration schemes for elastoplasticity coupled to anisotropic damage. *Applied Mechanics and Materials*, vol. 784, Trans Tech Publ, 2015; 217–224.

[16] Fassin M, Wulfinghoff S, Reese S. Application of an elastoplastic material model coupled with anisotropic damage for the failure prediction of a rocket combustion chamber wall. *Proceedings of the 6th European Conference for Aerospace Sciences (EUCASS)*, 2015.

[17] Wulfinghoff S, Fassin M, Reese S. Comparison of two time-integration algorithms for an anisotropic damage model coupled with plasticity. *Applied Mechanics and Materials*, vol. 784, Trans Tech Publ, 2015; 292–299.

[18] Bäker M, Fiedler T, Rösler J. Stress evolution in thermal barrier coatings for rocket engine applications. *Mechanics of Advanced Materials and Modern Processes* 2015; **1**(1):1–10.